LWP - 1021

LANGLEY WORKING PAPER

THE EFFECTS OF PARACHUTE SYSTEM MASS AND SUSPENSION-LINE ELASTIC PROPERTIES ON THE LADT #3 VIKING PARACHUTE INFLATION LOADS

By

Theodore A. Talay

and

Lamont R. Poole

Langley Research Center
Hampton, Virginia

NATIONAL AERONAUTICS AND SPACE ADMINISTRATION

December 30, 1971

LWP - 1021

December 30, 1971

LANGLEY WORKING PAPER

THE EFFECTS OF PARACHUTE SYSTEM MASS AND SUSPENSION-LINE ELASTIC PROPERTIES ON THE LADT #3 VIKING PARACHUTE INFLATION LOADS

Prepared By

Theodore A. Talay

Theodore A. Talay

and

Lamont R. Poole

Lamont R. Poole

Approved by Don D. Davis, Jr.

Don D. Davis, Jr., Chief
Space Technology Division

Approved for distribution by Robert H. Wright

for Clifford H. Nelson
Director for Space

LANGLEY RESEARCH CENTER

NATIONAL AERONAUTICS AND SPACE ADMINISTRATION

THE EFFECTS OF PARACHUTE SYSTEM MASS AND SUSPENSION-LINE ELASTIC PROPERTIES ON THE LADT #3 VIKING PARACHUTE INFLATION LOADS

By Theodore A. Talay and Lamont R. Poole

SUMMARY

Analytical calculations have considered the effects of 1) varying parachute system mass, 2) suspension-line damping, and 3) alternate suspension-line force-elongation data on the canopy force history. Results indicate the canopy force on the LADT #3 parachute did not substantially exceed the recorded vehicle force reading and that the above factors can have significant effects on the canopy force history.

INTRODUCTION

Several low altitude decelerator tests (LADT) of the Viking parachute have been conducted. In LADT #3 the parachute was being tested at 1.5 times its design load and failed before reaching full-inflation. From a knowledge of the data from this flight test it is the purpose of this document to investigate the canopy load history as compared to the recorded tensiometer (vehicle load) readings and specifically to study the effects of 1) enclosed and apparent mass, 2) suspension-line damping, and 3) differences between Langley Research Center and Goodyear Aerospace Company suspension-line static elastic data on the canopy load history.

Due to the fact that the LADT #3 decelerator failed before reaching full inflation, values of the tensiometer readings and projected area ratio have been extrapolated to a projected full-inflation time for use in this study. No attempt has been made to study the conditions past full inflation.

B.E.S. units are used throughout this document to simplify application of the results to the Viking project.

SYSTEM DESCRIPTION

The total deployment process for the Viking decelerator consists of an unfurling phase and an inflation phase as described in reference 1. Unfurling is the phase in which the parachute is strung out from the deployment bag in a lines-first manner following mortar fire. The canopy inflation phase is assumed to begin at the end of the unfurling process. Overall dimensions for the LADT #3 decelerator system are shown in figure 1. The distribution of weight along the parachute strung-out length is as presented in reference 1. Three different cases for the mass of the parachute system during inflation are considered. The first case is the parachute material mass only, the second the material mass plus the enclosed air mass and the third case has the material mass plus enclosed air mass plus the apparent air mass.

Suspension-line and bridle leg material force-elongation characteristics, as obtained at the Langley Research Center, are presented in figure 2. The suspension-line test data as obtained by the Goodyear Aerospace Company are presented later in this report.

Damping characteristics of the suspension-system material are presently undefined. For purposes of this analysis final results are compared for three values of damping to examine sensitivity. The bridle leg material is assumed to have zero damping and each leg is considered to have four layers of material for computation of force-elongation characteristics for the total bridle assembly.

The payload vehicle is a flared cylinder with a mass of 83.7 slugs.

Figure 1 gives the overall vehicle configuration.

SIMULATION AND RESULTS

Program Inputs

The unfurling sequence is simulated using the analytical model described in reference 2. Payload vehicle and decelerator physical properties are used as program inputs. Initial conditions at mortar fire were obtained from LADT #3 flight data. At mortar fire the Mach number was 0.33, the vehicle dynamic pressure was 24.09 pounds per square foot, and the flight path angle was equal to -63.0 degrees. The mortar velocity was adjusted until predicted line-stretch time was equal to that indicated by flight test data. The resulting conditions at bag strip were input into the inflation program.

The inflation sequence is simulated using a currently unpublished two-dimensional analytical model. The model considers nonlinear elastic properties and assumes a constant damping coefficient in calculating the damping force. As usual in most models of the elastic system, the weight of the canopy is considered attached to a massless spring-type suspension system. The vehicle, due to its streamlined shape and mass, is modeled as a no-drag point mass.

Geometry changes during inflation are prescribed by the canopy projected area ratio shown in figure 3 as obtained from LADT #3 test data. Because the LADT #3 parachute failed before reaching full inflation, an extrapolation of the curve to a probable time of full inflation is used.

In low altitude testing of the Viking decelerator, the enclosed and apparent air masses are considerably greater than the canopy mass alone, as in figure 4(a), while in high altitude testing these added air masses may be negligible compared to the canopy mass and thus omitted from the system mass without

affecting results. The significance of considering or neglecting these air masses in this low altitude drop test is investigated with three models.

These three models are 1) canopy material mass only, 2) canopy material mass plus enclosed air mass, and 3) canopy material mass plus enclosed air mass plus apparent air mass. The enclosed air mass history, the enclosed air mass plus apparent air mass history, and their time derivative histories for the LADT #3 decelerator as input into the analytical model are presented in figure 4. A separate program was developed to calculate these histories based upon the LADT #3 test air density and projected-area ratio.

In addition to zero damping for the case of the parachute with enclosed plus apparent air mass, values of a constant damping coefficient of 25 pound-seconds per suspension-line and 50 pound-seconds per suspension-line were employed. This coefficient is the ratio of the force caused by damping to the strain rate (in percent per second).

The drag area (C_DS) histories for all of the cases considered were obtained by using an unpublished prediction technique which, basically, involves a reversal of the two-dimensional analytical model in which LADT #3 tensiometer (vehicle force) data were input and a C_DS history was computed. An extrapolation of the tensiometer flight data from the failure point to the predicted time of full inflation gave the full inflation tensiometer value. The C_DS history represents that forcing function input necessary to obtain the predicted vehicle force equal to the flight (tensiometer) vehicle force. As different models are considered, different C_DS histories are required. Separate C_DS histories for the three different parachute system masses, three different values of damping (including zero damping), and two sets of suspension-line force-elongation data were computed and used to obtain the resulting canopy

load histories.

Program Results

Unfurling sequence.- The time between mortar fire and line stretch is 0.88 seconds. A mortar velocity of 109 ft/sec is required to match program line-stretch time to flight data as shown in figure 5. The total unfurling time between mortar fire and bag strip is 1.13 seconds. Inflation is assumed to begin at bag strip.

Inflation sequence.- At the beginning of inflation the Mach number is 0.36, the vehicle dynamic pressure 29.25 pounds per square foot, and the flight path angle -65.70 degrees.

The first effect studied is that of varying the parachute system mass. Figure 6 presents the C_DS histories required to obtain predicted vehicle load histories equal to the recorded (tensiometer) vehicle load history. These C_DS histories are input into the analytical inflation model and the results are presented in figures 7, 8, and 9. Figure 7 represents the case where only the canopy material mass is employed. Figure 8 represents the canopy material mass plus enclosed mass case and figure 9 represents the canopy material mass plus enclosed mass plus apparent mass case. Zero damping is assumed for these three cases. In all three cases, figures 7(a), 8(a), and 9(a), the predicted vehicle dynamic pressure history closely approximates the values obtained from flight data. The computed vehicle force histories, figures 7(b), 8(b), and 9(b), also agree well with the flight vehicle force.

The results indicate that up to the point of LADT #3 failure at 1.70 seconds past mortar fire, the effect of adding additional mass to the parachute system is to decrease the computed canopy force. This can be explained by the interplay between the canopy force and the product of the additional air mass flow

rate amd the canopy velocity. Similar conclusions were reached in reference 4.

In figure 7(b), the case of canopy material mass only, the canopy force follows the vehicle force closely. At the point of LADT #3 failure, at 1.70 seconds, the canopy force is equal to the vehicle force. In figure 8(b), the case of canopy material mass plus enclosed air mass, the canopy force is, at all points up to 1.70 seconds, markedly less than the vehicle force. At the failure point, the canopy force is approximately 4.1% below the vehicle force. In figure 9(b), the case of canopy material mass, enclosed air mass, and apparent air mass, the canopy force is, up to 1.70 seconds, again markedly less than the vehicle force. At the failure point the canopy force is approximately 0.7% below the vehicle force. At predicted full inflation the canopy force is greater than the vehicle force in all cases. The calculated difference is 1.1%, 4.9%, and 5.2% for the three cases respectively in figures 7(b), 8(b), and 9(b).

The second effect studied is that of damping. A parachute system mass which includes the enclosed air mass and apparent air mass is used with constant damping coefficient values of 0, 25, and 50 pound-seconds per suspension-line. Figure 10 presents the C_DS histories required to obtain predicted vehicle load histories equal to the recorded (tensiometer) vehicle load history. These C_DS histories were input into the analytical inflation model and the results are presented in figures 9, 11, and 12. Again, as in the varying parachute system mass cases, the predicted vehicle dynamic pressure histories closely approximate the values obtained from flight data and the computed vehicle force agrees well with the flight vehicle force. The major effects of damping are to change the shape of the canopy force history and to increase the canopy force at the failure point and at full inflation. Figure 9 was discussed previously as the final case in the varying parachute mass study. In figure 11(b), the

damping coefficient is 25 pound-seconds per suspension-line. Up to approximately 1.5 seconds the canopy force history levels out more than that of the no damping case. The leveling out effect is even more pronounced in figure 12(b), the case of the damping coefficient equal to 50 pound-seconds per suspension line. At the LADT #3 failure time of 1.70 seconds the canopy force is 0.8% and 2.4% greater than the vehicle force for the two respective damping coefficients. At full inflation the canopy force has increased to 7.8% and 10.6% greater than the vehicle force for the two respective damping coefficients used.

The final effect investigated was that due to differences in the Viking suspension-line static force-elongation data obtained by Langley Research Center and Goodyear Aerospace Company and presented in figure 13. The LRC samples tested were unsterilized while those tested at GAC were sterilized, which may explain the differences observed. The case used for comparison was that of canopy material mass plus enclosed air mass plus apparent air mass, with zero damping. The only change was substituting the GAC suspension-line data for the LRC data. Figure 14 presents the C_DS histories required to obtain predicted vehicle load histories equal to the recorded (tensiometer) vehicle load history. These histories were input into the analytical inflation model and the results are presented in figures 9 and 15. The predicted vehicle dynamic pressures, figures 9(a) and 15(a), are close to the values obtained from flight data and the computed vehicle force agrees well with the flight vehicle force. While it is noted that in comparing the two canopy force histories, figures 9(b) and 15(b), some difference is present early in the inflation sequence, it is also observed that much lower values of canopy force occur at the LADT #3 failure point and full inflation point using GAC data. At the failure point the canopy force is 15.7% below the vehicle force and at the predicted full inflation point the canopy force is

1.8% above the vehicle force.

The following table summarizes the results obtained from this study at the LADT #3 failure time and the predicted full inflation time:

MAGNITUDE OF CANOPY FORCE RELATIVE TO VEHICLE FORCE FOR LADT #3

Conditions	Failure Time 1.70 sec	Predicted Full Inflation Time 1.80 sec
Canopy mass, no damping	0	+1.1%
Canopy mass plus enclosed mass, no damping	-4.1%	+4.9%
Canopy mass plus enclosed mass plus apparent mass, no damping	-0.7%	+5.2%
Same, 25 damping	+0.8%	+7.8%
Same, 50 damping	+2.4%	+10.6%
Same, 0 damping, GAC line data	-15.7%	+1.8%

CONCLUSIONS

Analytical calculations have considered the effects of 1) varying parachute system mass, 2) suspension line damping, and 3) different suspension-line force-elongation data on the canopy force history. Based on the results of this study the following conclusions are drawn:

Specifically,

1. At the LADT #3 failure time of 1.70 seconds, the canopy force ranged anywhere from 15.7% below to 2.4% above the vehicle force depending upon the model and data used. Therefore, the canopy force did not substantially exceed

the recorded vehicle force reading.

2. At a predicted full inflation time of 1.80 seconds the canopy force would be greater than the vehicle force by from 1.1% to 10.6%, again depending upon the model and data used.

Generally,

3. At low altitudes, enclosed and apparent air mass can significantly effect the canopy force calculated and should, therefore, not be neglected.

4. The canopy force calculations are sensitive to decelerator physical properties. In this case changes in the damping and/or force-elongation characteristics produced significant changes in the canopy force histories. Accurate prediction of canopy force histories requires accurate inputs in these areas.

REFERENCES

1. Talay, Theodore A.; Poole, Lamont R.; and Whitlock, Charles H.: The Effect of Suspension-Line Length on Viking Parachute Inflation Loads. LWP-985, Sept. 1971.

2. Poole, Lamont R.; and Huckins, Earle K. III: Evaluation of Massless-Spring Model of Suspension-Line Elasticity during the Parachute Unfurling Process. Prospective NASA TN.

3. Goodyear Aerospace Corp. Drawings No. 3064130-102 and 3064110-104.

4. Heinrich, H.G.; and Noreen, R.A.: Analysis of Parachute Opening Dynamics with Supporting Wind-Tunnel Experiments. Journ. of Aircraft, July-August 1970.

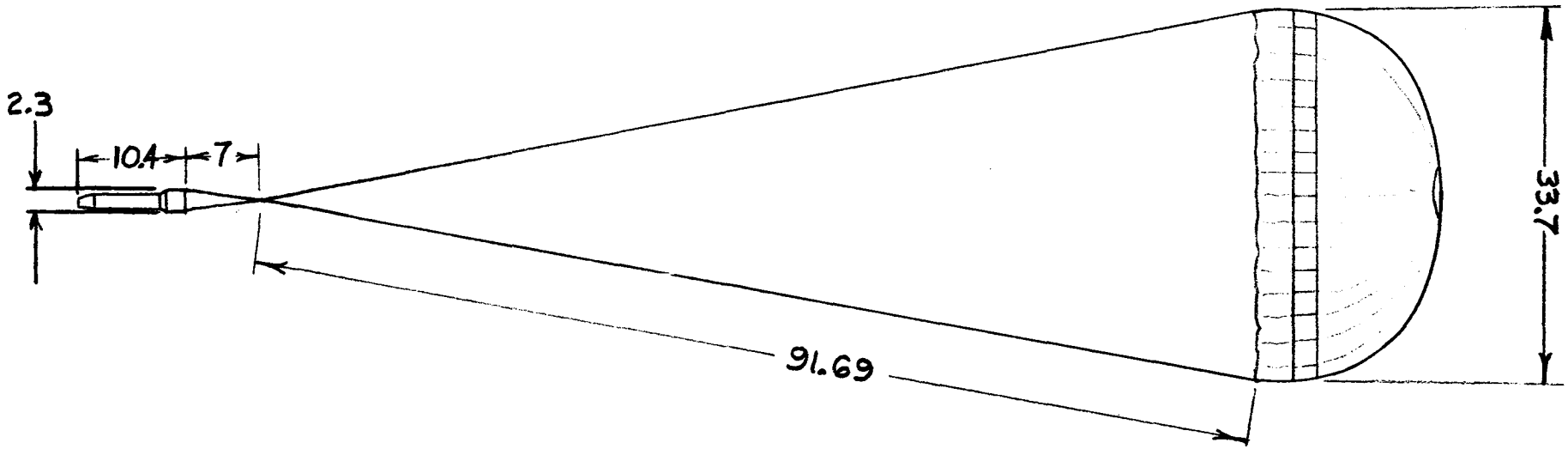

Figure 1.– Sketch of general LADT configuration (dimensions in feet).

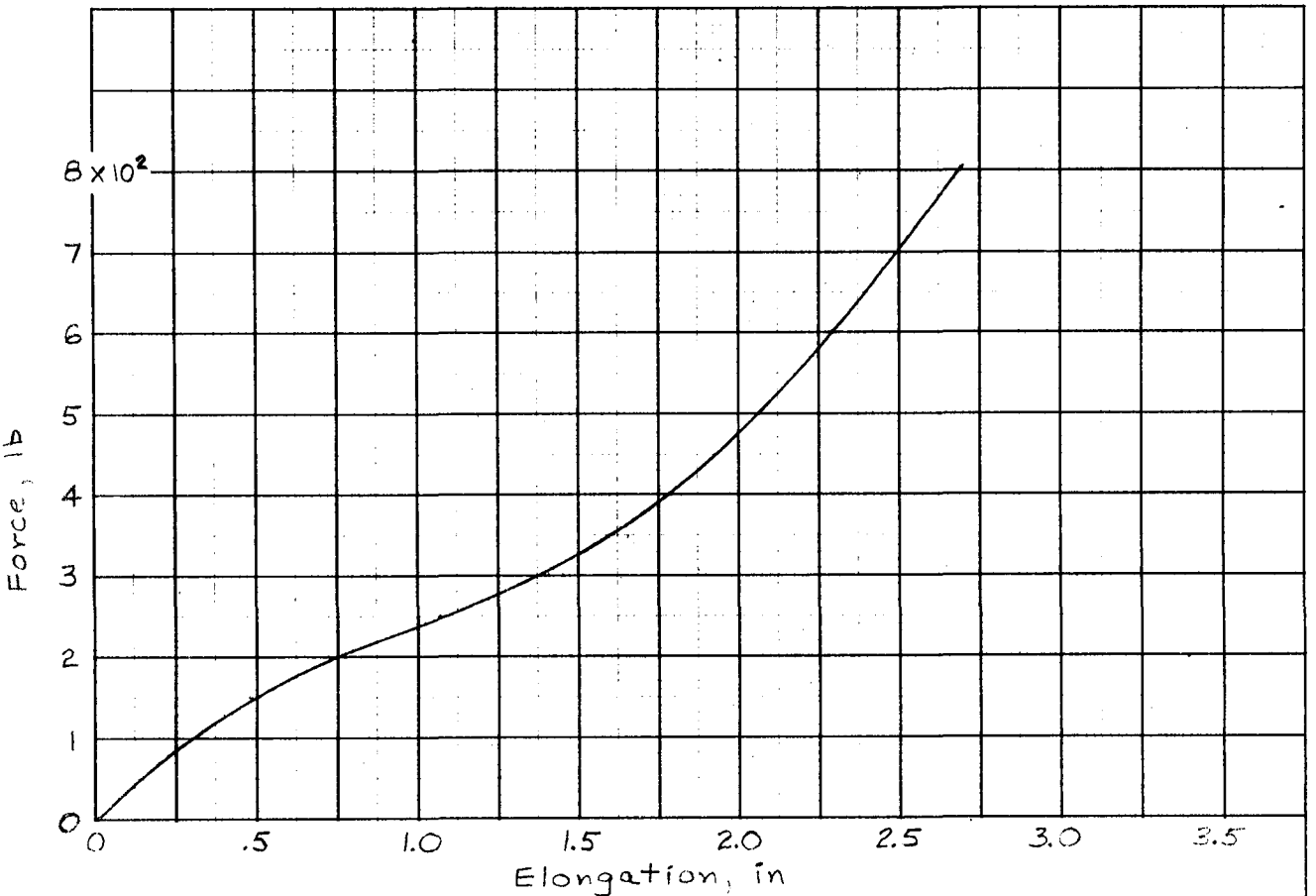

(a)- Viking suspension line sample

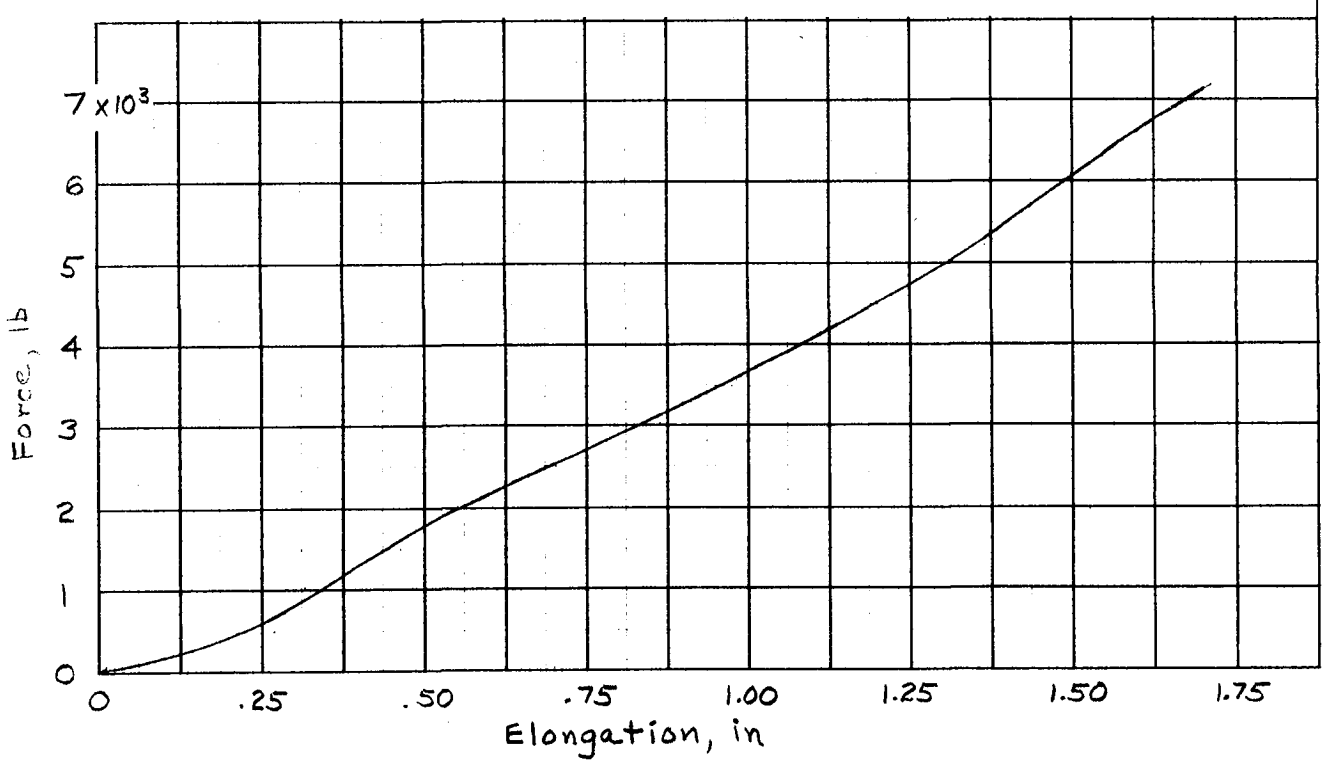

(b)- Viking bridle material sample

Figure 2.- Force-elongation curves for Viking suspension line and bridle samples, as obtained from Instron tests (gage length ≅ 10 in).

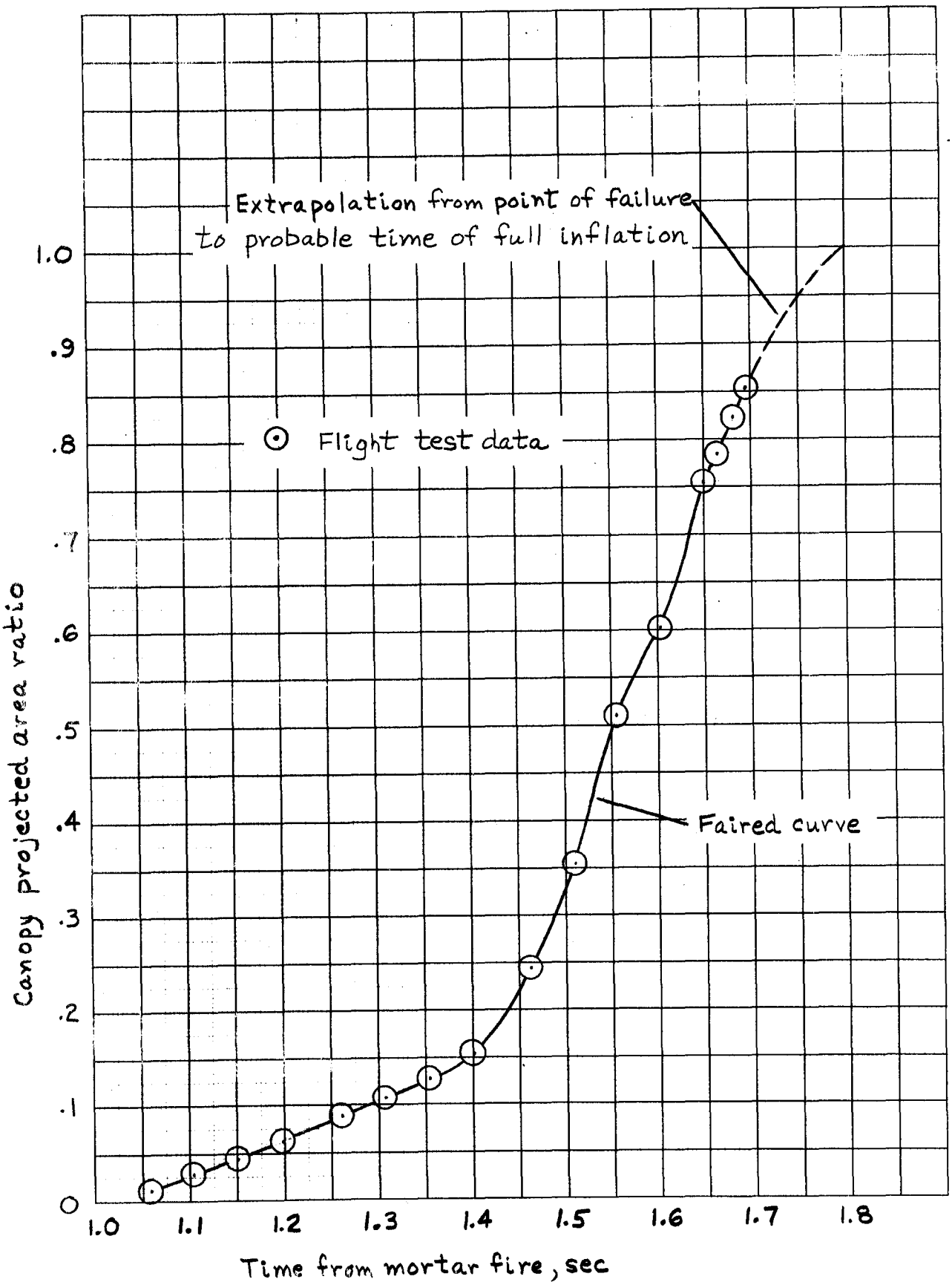

Figure 3.- Input history of canopy projected area ratio for LADT #3.

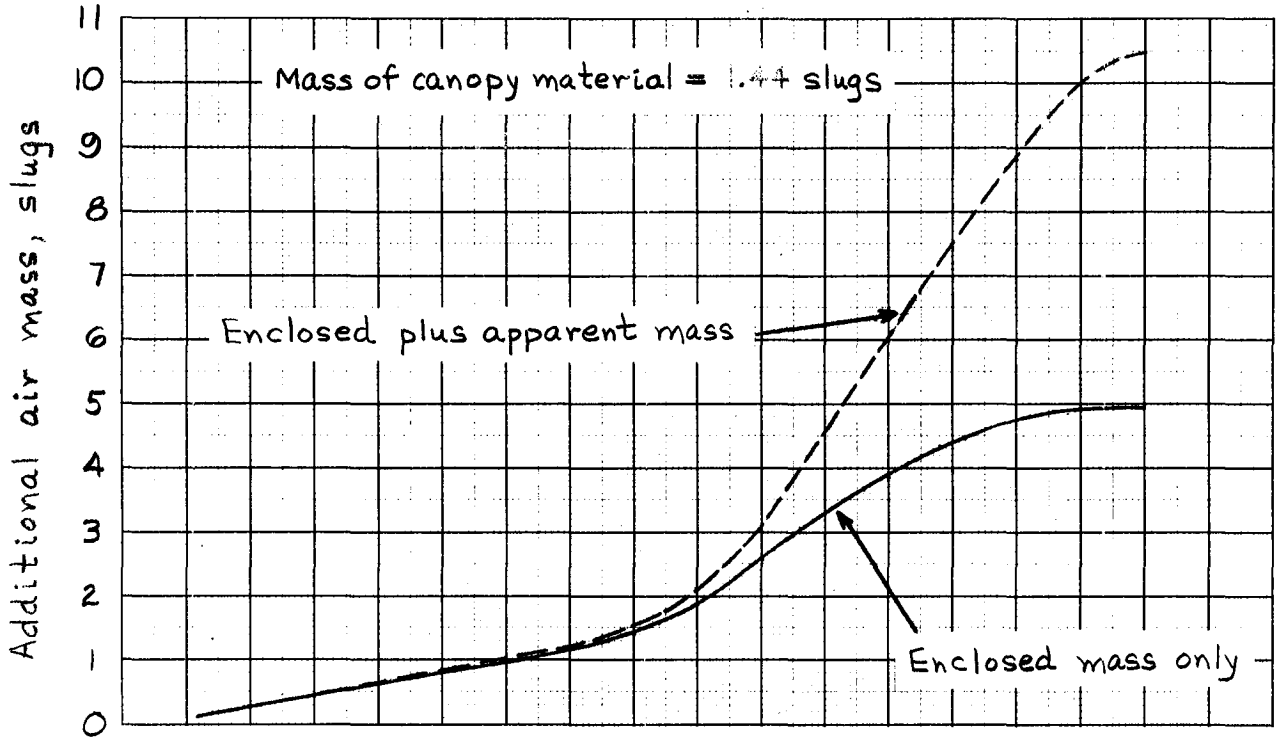

(a) Additional air mass history

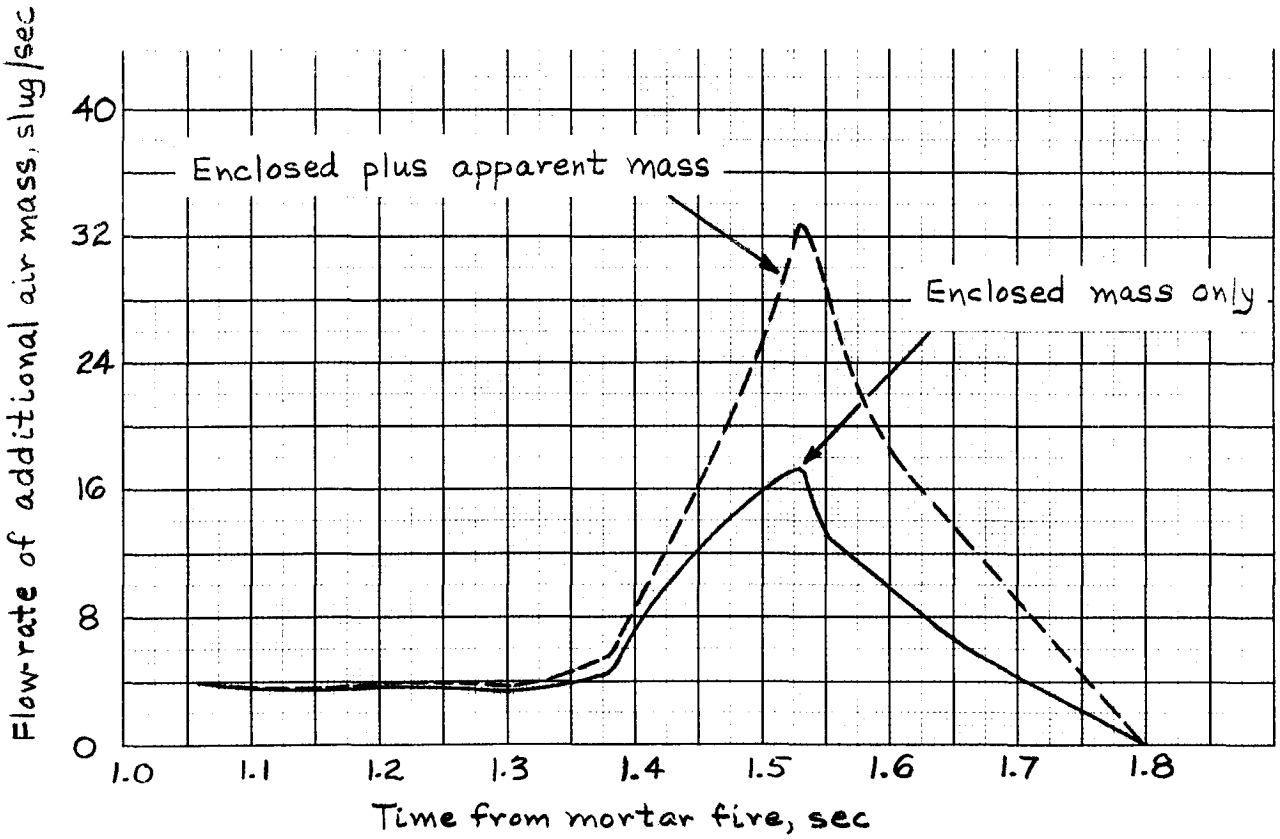

(b) Flow-rate of additional air mass

Figure 4.- Input histories of additional air mass and air mass flow rates for LADT # 3.

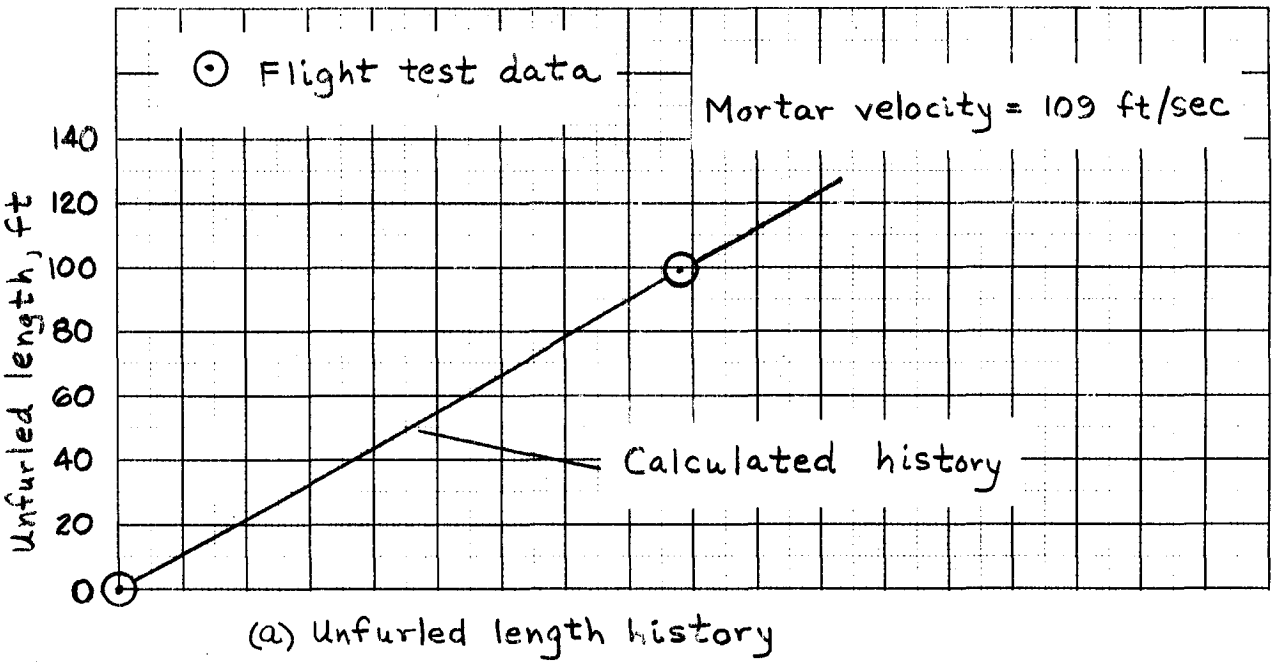

(a) Unfurled length history

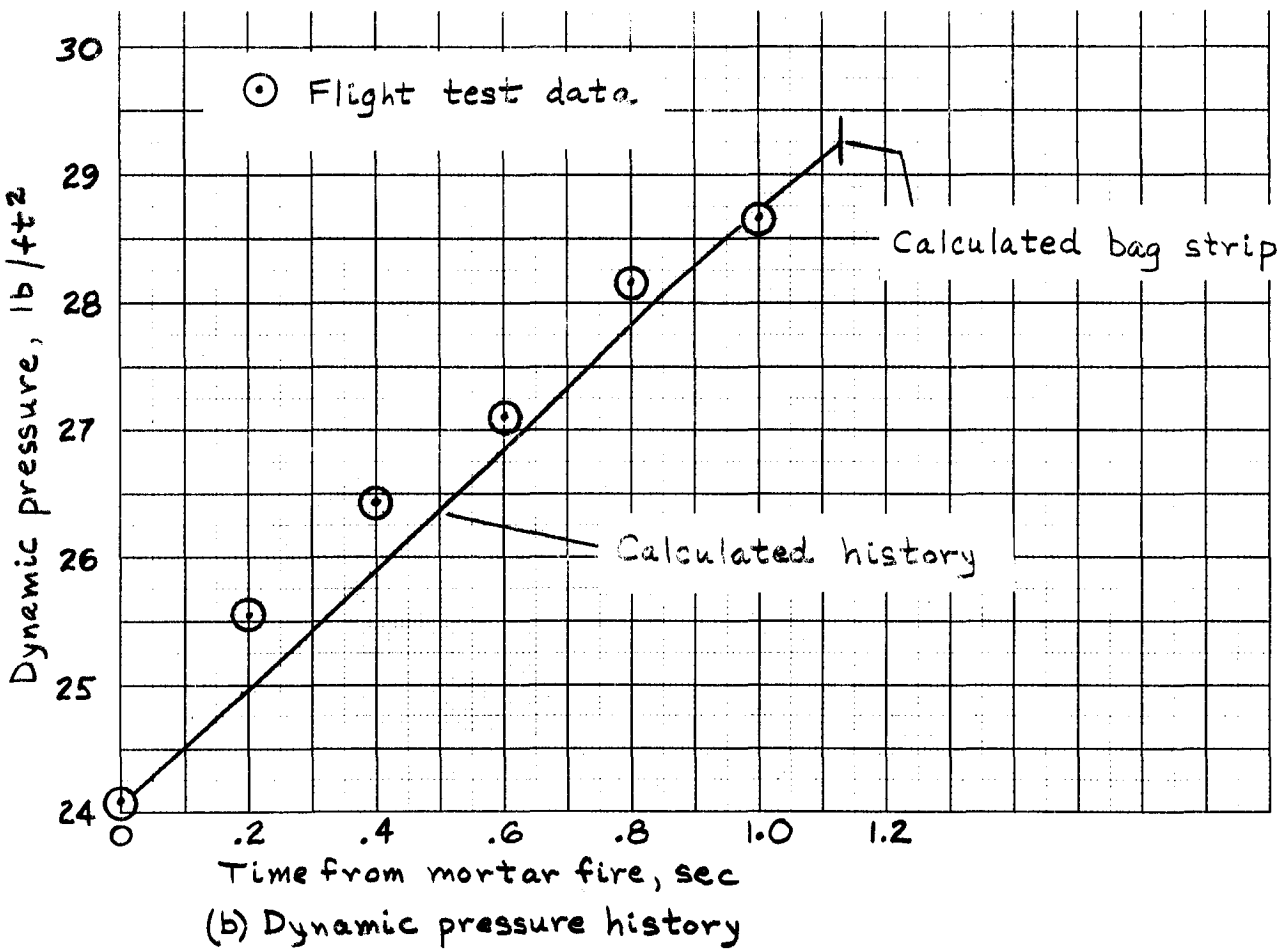

(b) Dynamic pressure history

Figure 5.- Comparison of flight data and calculated histories of unfurled length and dynamic pressure.

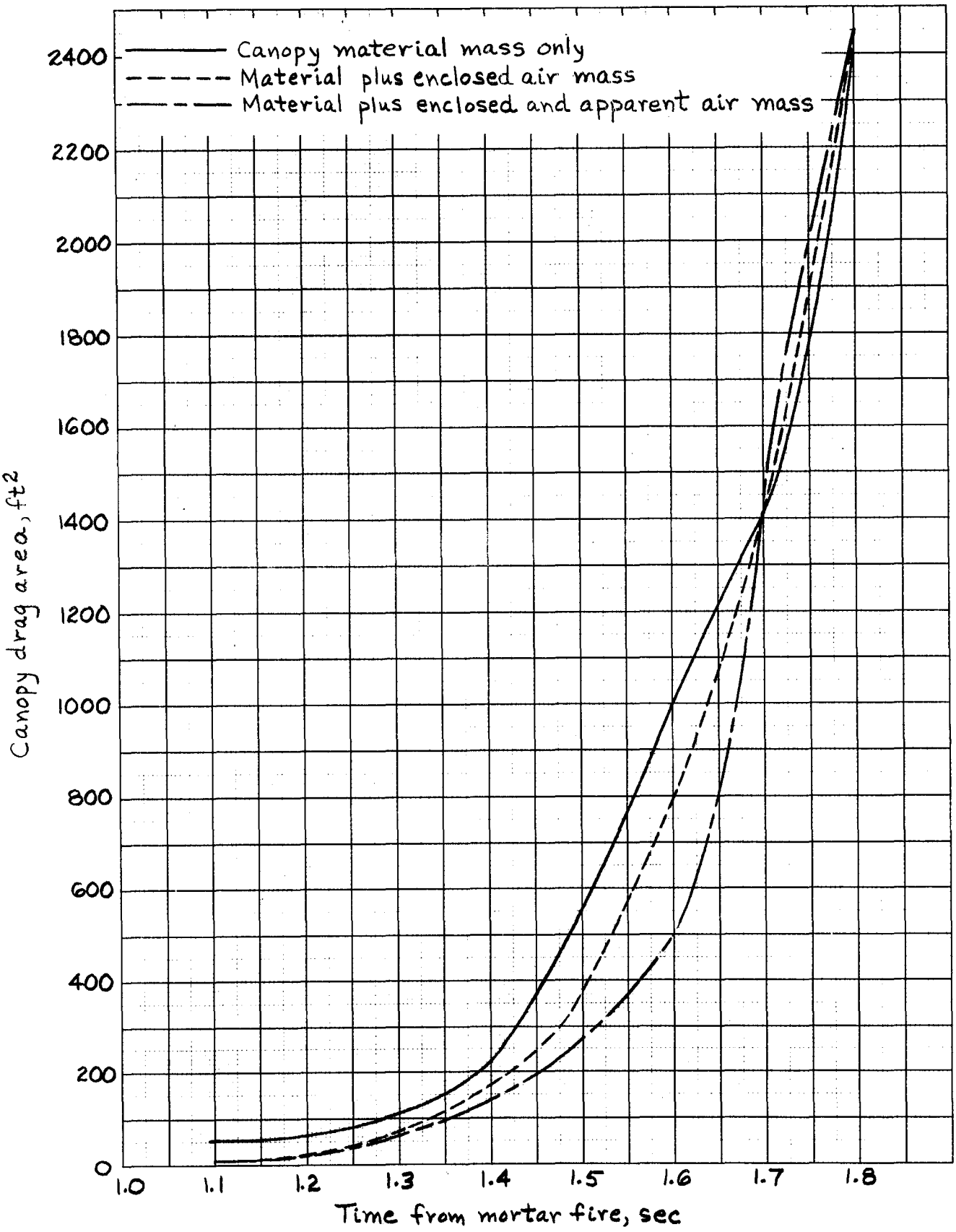

Figure 6.- Input histories of canopy drag area for three canopy mass conditions of LADT #3.

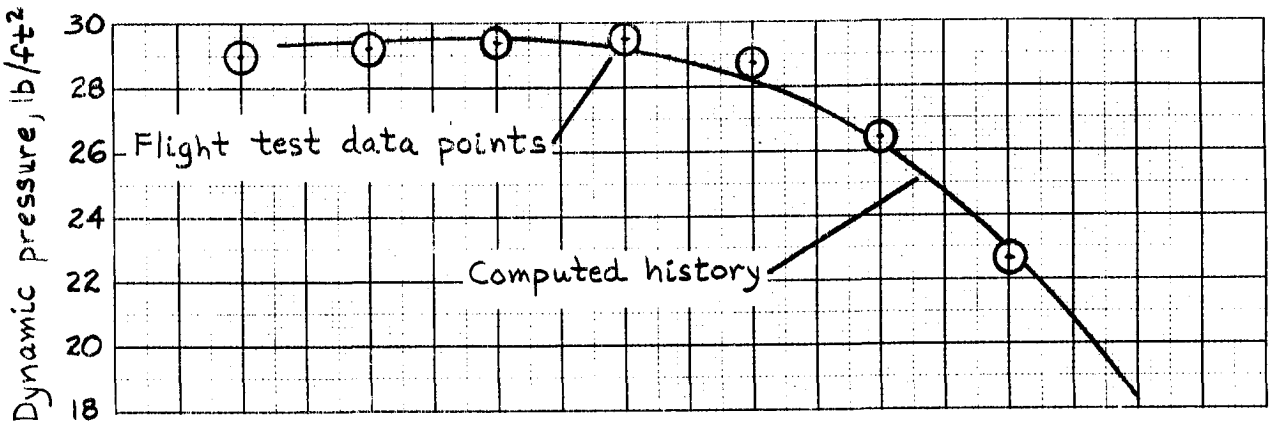

(a) Dynamic pressure history

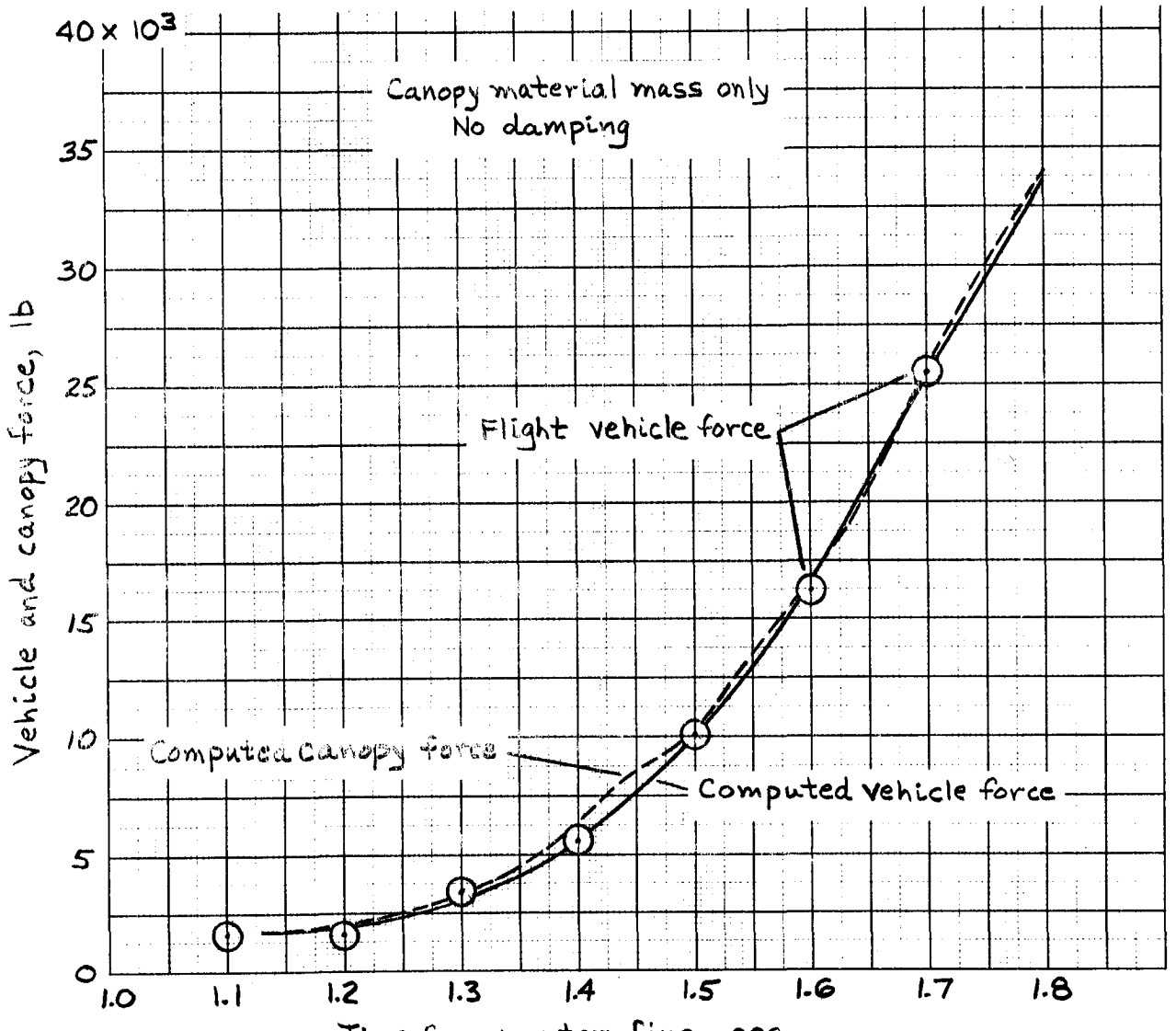

(b) Vehicle and canopy force histories

Figure 7 .- Comparison of computed and actual histories of dynamic pressure and force for LADT # 3; material mass only ; damping coefficient = 0.

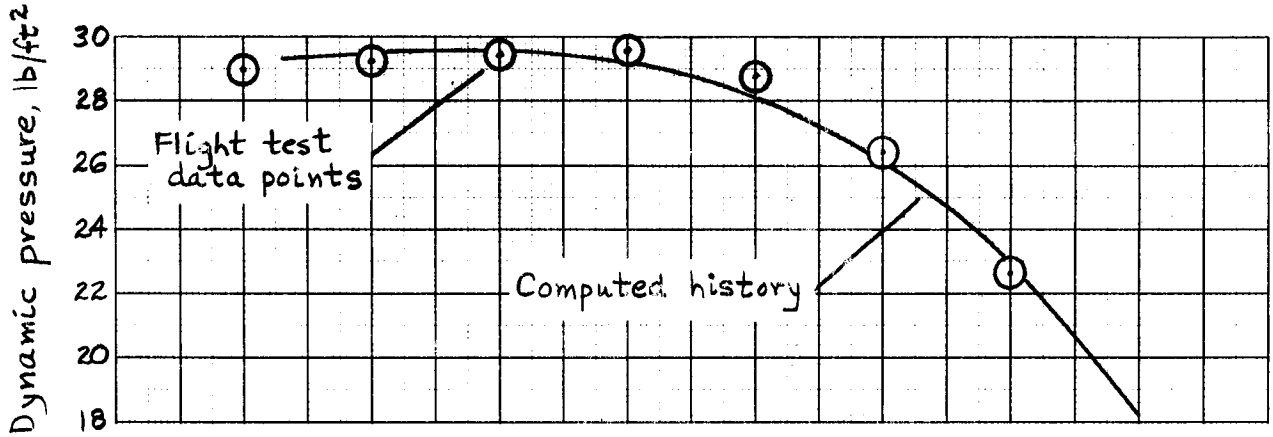

(a) Dynamic pressure history

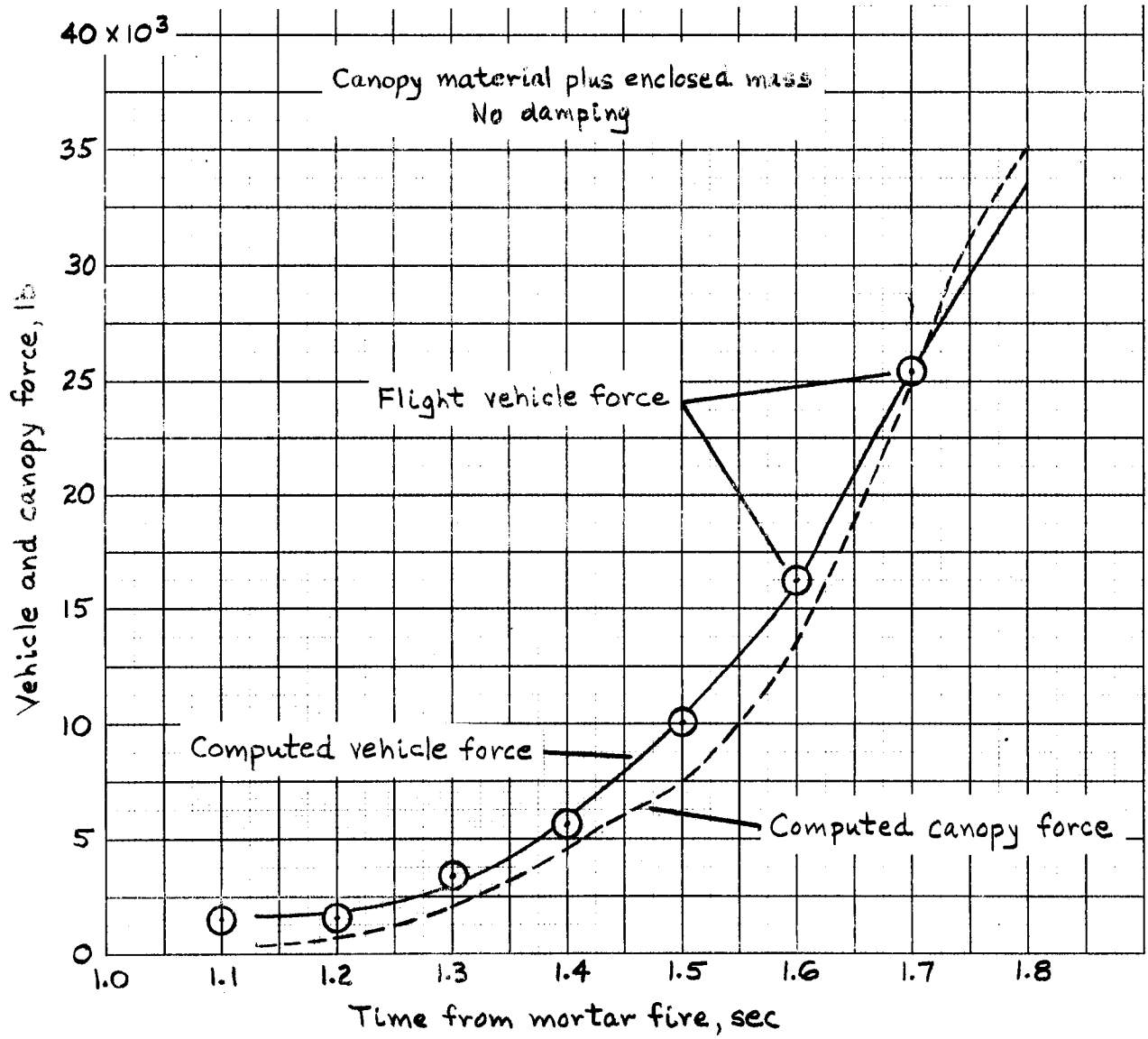

(b) Vehicle and canopy force histories

Figure 8.- Actual and computed histories of dynamic pressure and force for LADT # 3; canopy material plus enclosed mass; damping coefficient = 0.

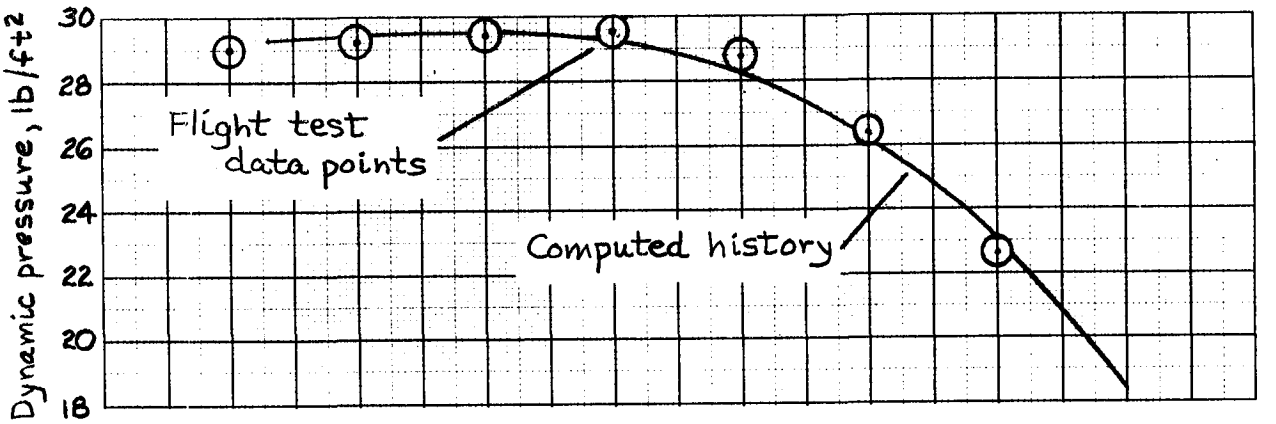

(a) Dynamic pressure histories

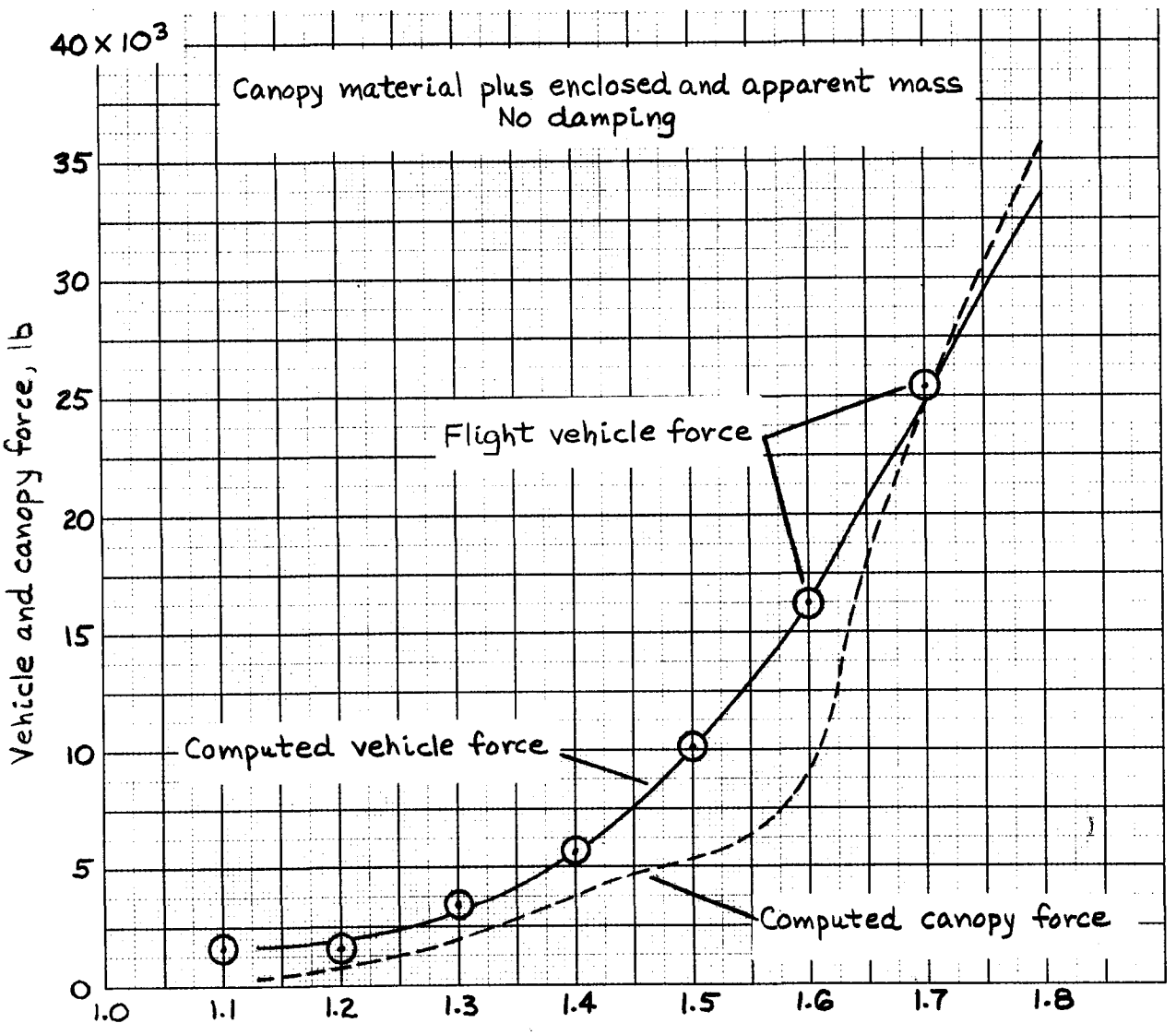

(b) Vehicle and canopy force histories

Figure 9.– Actual and computed histories of dynamic pressure and force for LADT #3; material plus enclosed and apparent mass; damping coeff. = 0.

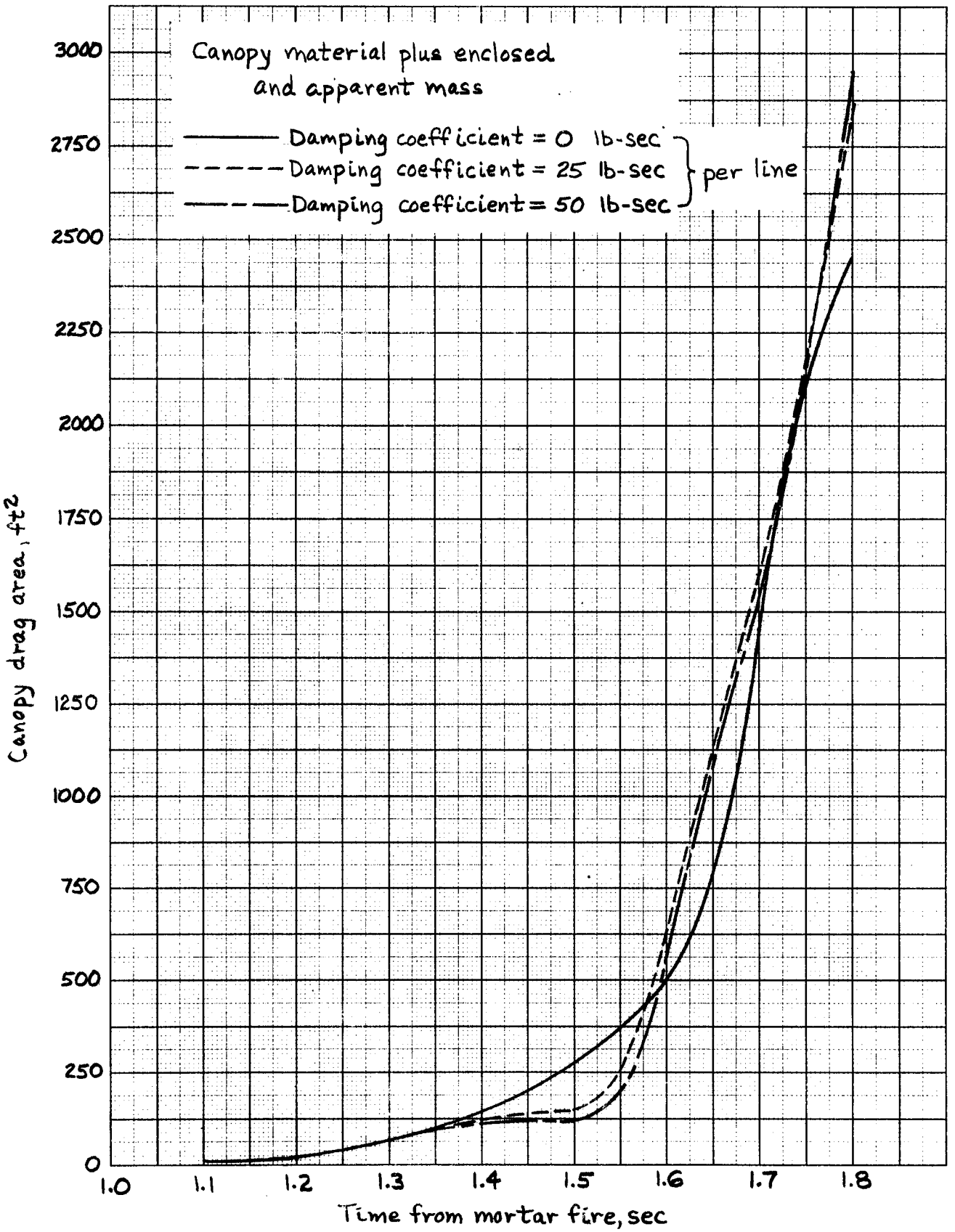

Figure 10.- Input histories of canopy drag area for comparative damping cases of LADT #3.

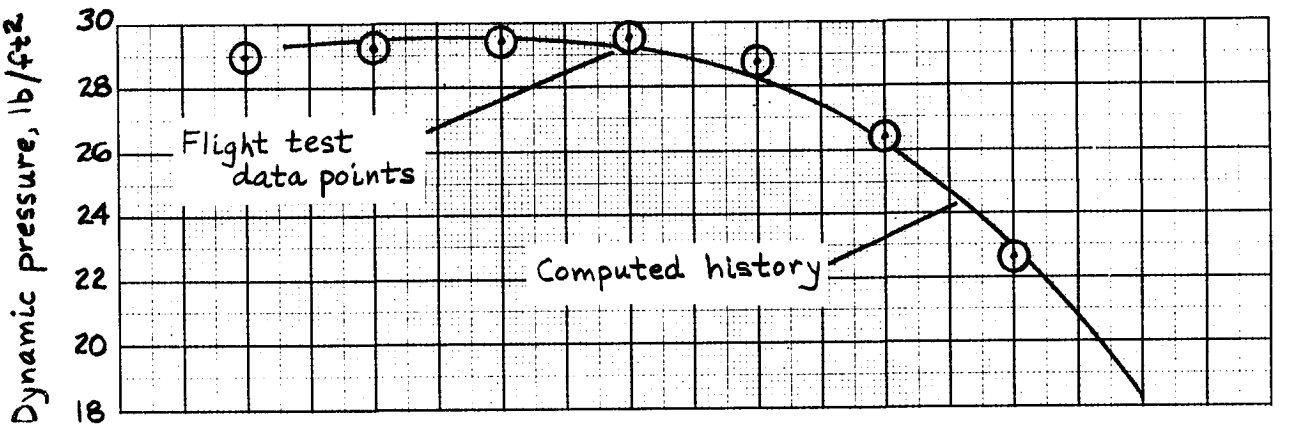

(a) Dynamic pressure histories

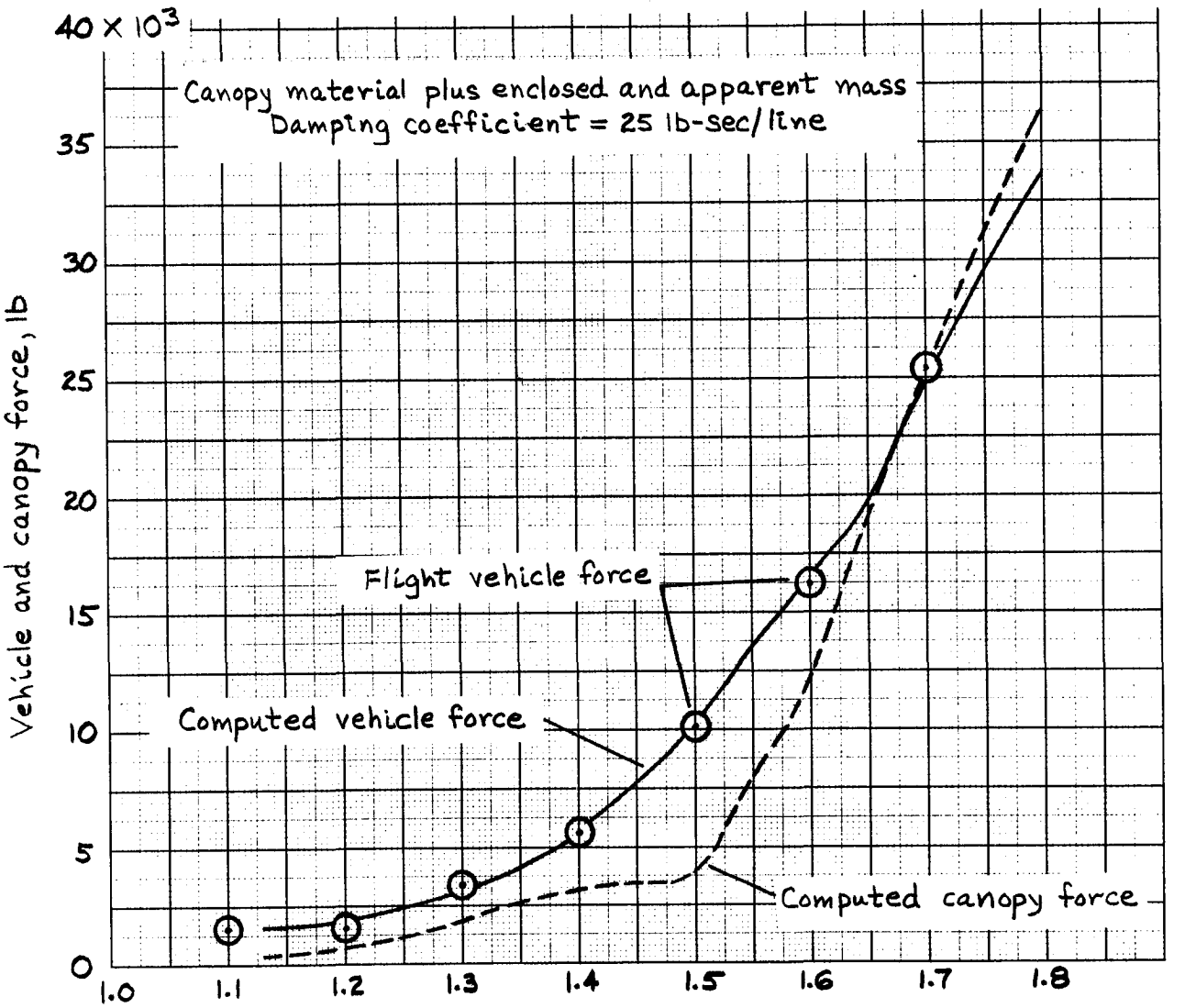

(b) Vehicle and canopy force histories

Figure 11.– Actual and computed histories of dynamic pressure and force for LADT#3; material plus enclosed and apparent mass; damping coeff. = 25.

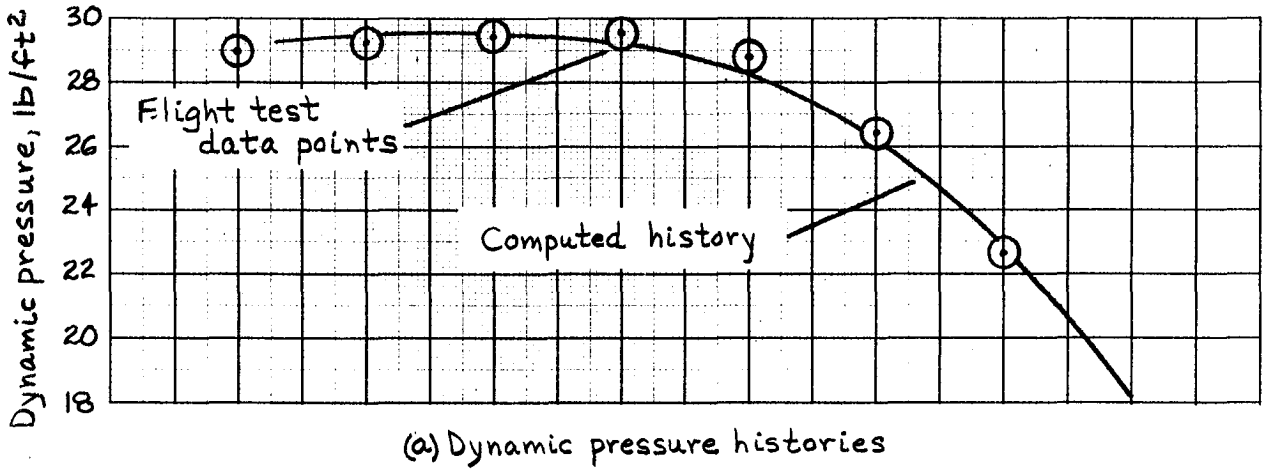

(a) Dynamic pressure histories

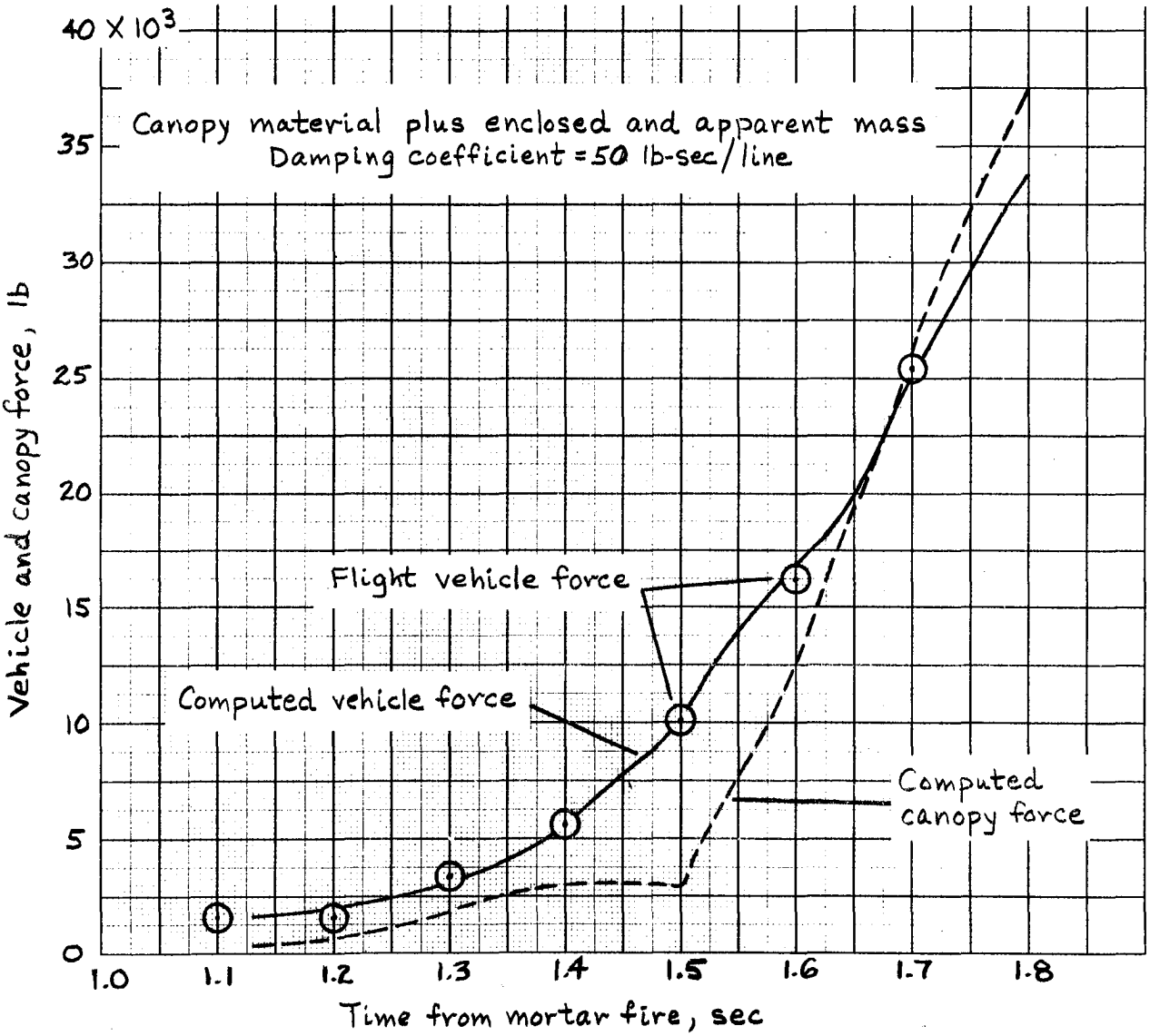

(b) Vehicle and canopy force histories

Figure 12.– Actual and computed histories of dynamic pressure and force for LADT #3; material plus enclosed and apparent mass; damping coeff. = 50.

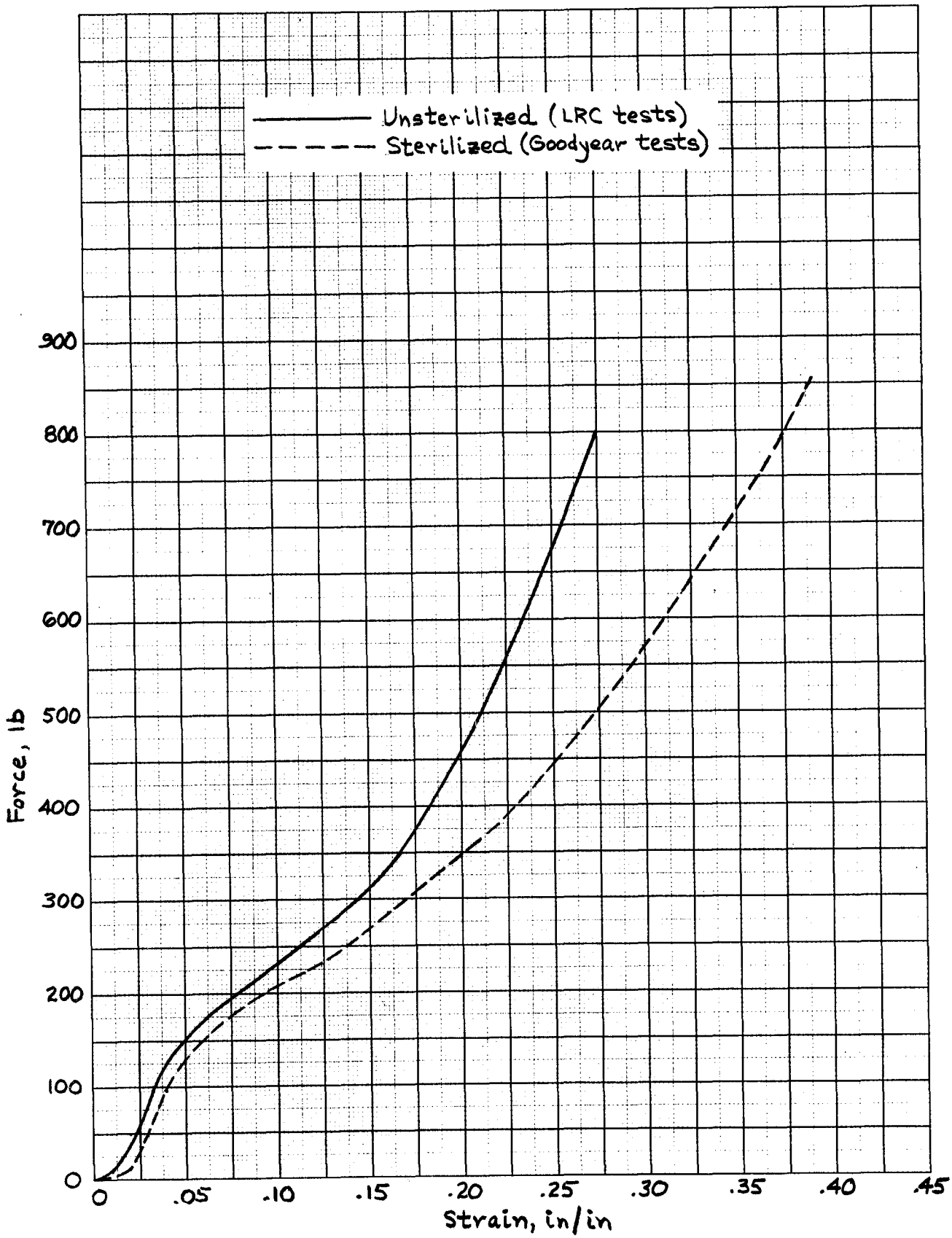

Figure 13.- Comparison of force/strain curves for sterilized and unsterilized samples of Viking suspension line material.

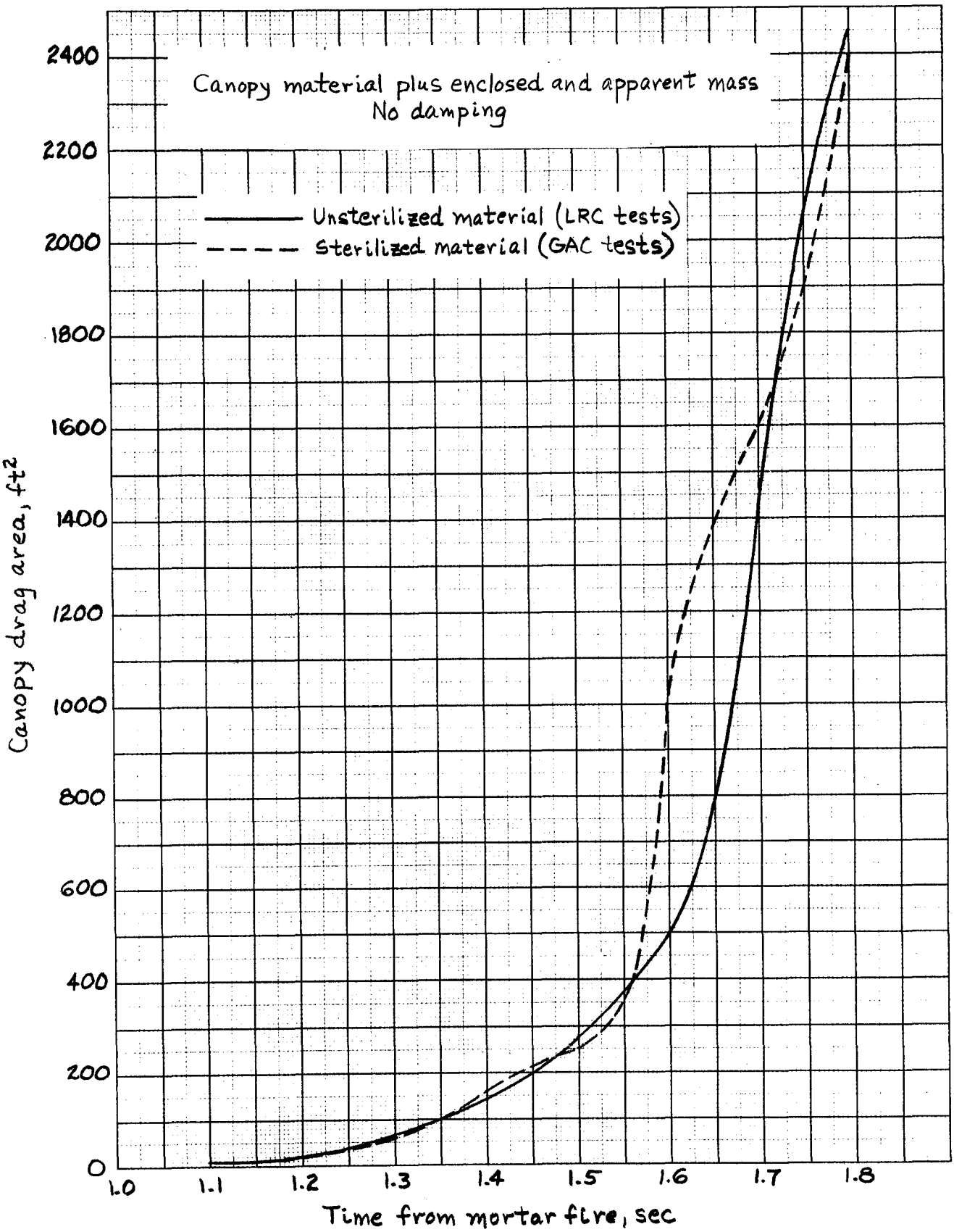

Figure 14.– Input histories of canopy drag area for two suspension-line elasticity cases of LADT #3.

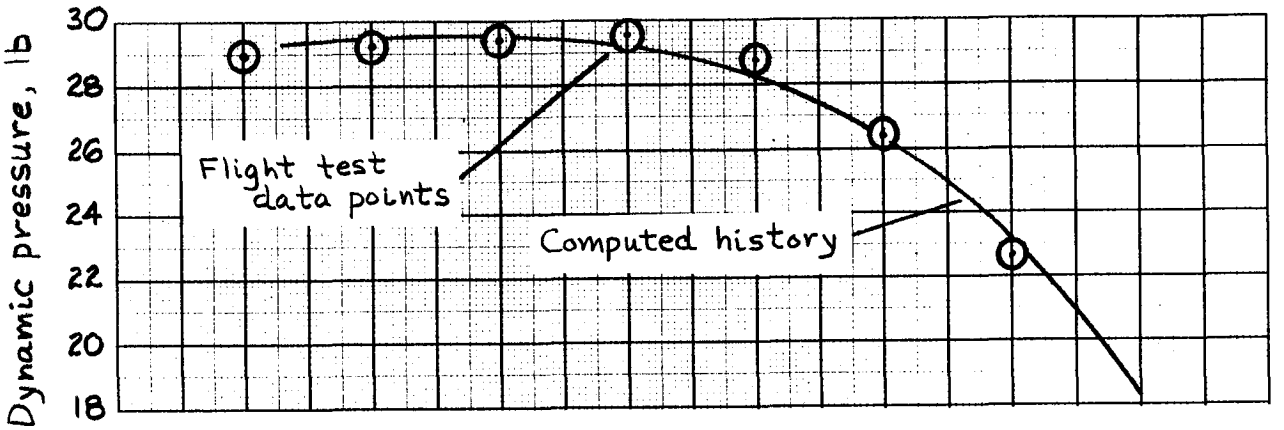

(a) Dynamic pressure histories

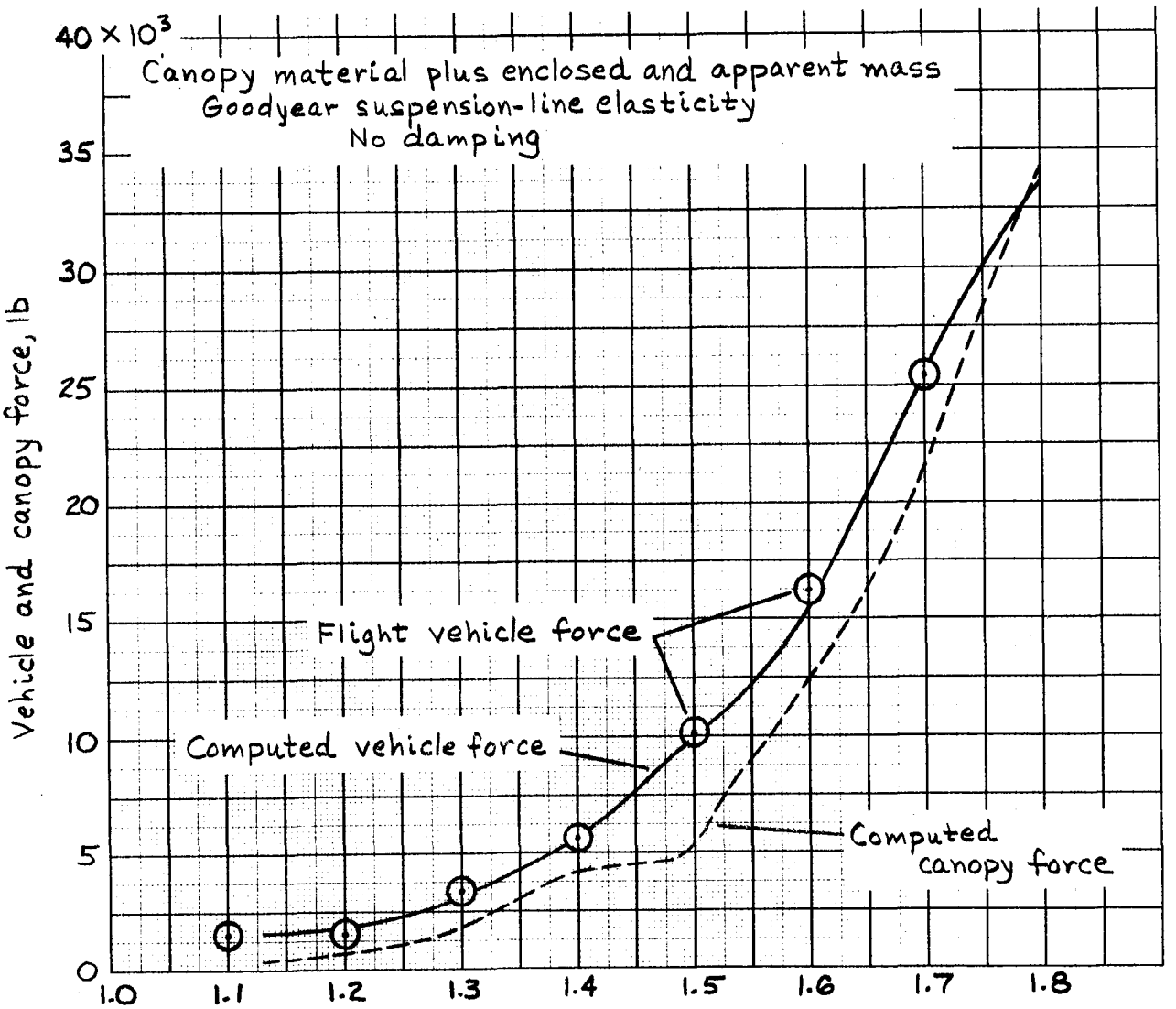

(b) Vehicle and canopy force histories

Figure 15.- Actual and computed histories of dynamic pressure and force for LADT #3; canopy material plus enclosed and apparent mass; GAC elasticity.